Design of Variable Traffic Light Control Systems for Preventing Two-Way Grid Network Traffic Jams Using Timed Petri Nets

Jiliang Luo, *Senior Member, IEEE*, Yi-Sheng Huang, *Senior Member, IEEE*, and Yi-Shun Weng

***Abstract*— Cell transmission model (CTM) is useful for evaluating the performance of urban traffic networks due to its mathematical formalism. This paper explores the application of CTM to develop control strategies for dispersion accident-induced traffic jams and evaluates the efficiency of these strategies. On the other hand, Timed Petri nets (TPNs) perform in discrete event systems because they provide a balance between modeling power and analyzability. This paper focuses on using the developed TPNs to model variable traffic light control systems. One advantage of the proposed methods is that the traffic light behavior is clearly represented in terms of conditions and events, which result in changes in the pre-emption phase. Moreover, this paper also proposes a new control strategy to eliminate the traffic jam propagation by preventing the traffic flow heading in the direction of an accident. The analysis is performed to demonstrate how the models enforce the phase of traffic transitions by a reachability graph with time information. The liveness and reversibility of the proposed model are verified. To the best of our knowledge, this is the first paper to use TPNs to model a variable phase traffic light control system and identify its accident scenarios for the purpose of their complete avoidance. This helps the latest advanced technology in traffic safety related to the intersection of roadways.**

***Index Terms*— Cell transmission model (CTM), traffic jam, Timed Petri net (TPN), traffic light, traffic safety.**

I. Introduction

TRAFFIC congestion is a growing problem in many big cities because a growing number of vehicles are used. With more and more vehicles, the transportation delay and traffic congestion on urban arterials are increasing throughout the world. Hence, it is essential to possess strategic analysis methods for increasing the efficiency of transportation. Intelligent transportation system (ITS) can play an important role in improving transportation system efficiency and safety. Naturally, ITS technologies are applied in traffic congestion issues, such as traffic accident detection and verification [1]–[3], accident response logistics [4], and accident wireless communication [5]. Besides, Figueiredo *et al.* [6] analyze the freeway traffic via a simulator of ITSs. On the other hand, the problem of traffic congestion has become a major issue, particularly when a car crash occurs in an urban area.

Car accidents can cause traffic jams that spread over large tracts of an urban network. Consequently, one demands to study the process of traffic jam formation and growth. We understand that a traffic jam can be caused by one of the following three reasons [7]: (1) a temporary obstruction, (2) a permanent capacity constraint, and (3) a stochastic fluctuation in the demand. Here, we only pay attention to traffic congestion caused by a grid network accident that might be categorized under (1) or (2). Qi *et al.* [8] pointed out that accident-based congestion is a kind of traffic jam. If the accident is not cleared in time, it may lead to large-scale congestion of upstream traffic. Much research work has been discussed with various accident-based jam issues, such as Wright and Roberg [7] proposed a simple analytical model and Roberg [9] proposed accident simulation models, are based on accident-based jam formation and growth. Additionally, Roberg-Orenstein *et al.* [10] mentioned that the accident-based control strategy can be divided into static prevention and dynamic control strategies. The static prevention strategy issues on how the road layout features can be employed to diminish the jam spreading. The dynamic control strategy can be hired to slow the jam propagation. Daganzo [11] proposed CTM for analyzing network traffic and the method can be applied to solve the problem of traffic jams. Recently, Long *et al.* [12] stated that CTM can simulate network-wide traffic flow in a more realistic manner than traffic flow in one-way networks [9], [13]–[15]. Especially, they have extended CTM and employed it to simulate accident-based jam propagation in two-way grid networks. Moreover, two-way roads are more commonly found in urban traffic networks than one way ones [16]. Nevertheless, Qi *et al.* [8] also proposed control strategies for dispersion accident-induced traffic jams and evaluated the efficiency of these strategies. On the other hand, Roberg-Orenstein *et al.* [10] have developed various strategies to solve traffic congestion issues.

A lot of work has been invested into developing various traffic signal control strategies to improve traffic efficiency. They are divided into three categories: (1) fixed-timed, (2) traffic responsive and (3) predictive control strategies. The first one is widely adopted in most existing urban transportation systems

Manuscript received February 23, 2019; revised May 28, 2019; accepted June 21, 2019. This work was supported in part by the National Science Council of Taiwan under Grant MOST 107-2221-E-197-026 and in part by the Natural Science Foundation of China under Grant 61573158. The Associate Editor for this paper was M. Zhou. *(Corresponding author: Yi-Sheng Huang.)*

J. Luo is with the College of Information Science and Engineering, Huaqiao University, Xiamen 361021, China.

Y.-S. Huang is with the Department of Electrical Engineering, National Ilan University, Yilan 260, Taiwan (e-mail: yshuang@niu.edu.tw).

Y.-S. Weng is with the Department of Electronic Engineering, Army Academy, Taoyuan 32093, Taiwan.

Digital Object Identifier 10.1109/TITS.2019.2925824

because it is easy to implement and manage. However, the drawback of fixed-timed is based on historical traffic flow data rather than real-time data. The second one, such as Li *et. al* apply the deep reinforcement learning method to find a better signal timing planc [17]. The third one is an optimal control strategy that predicts the future traffic behavior of the network [18]. Moreover, two traffic light strategies are proposed for single-intersection control and network-wide control, such as minimizing the queue lengths described by an optimal traffic light switching scheme model [19] and applying the network-wide traffic control in large-scale [20]–[26]. Unfortunately, most of the existing control strategies are only suitable for low/middle traffic flow and stable conditions. Note that an accident can quickly invalidate the above control strategies due to traffic congestion. In order to solve the problem of urban traffic jams based on accidents, mostly prevented methods are adopted traffic flow diversion with the help of the traffic police. Usually, ban traffic signals are adopted [9], [16] to notify road users might not enter traffic jam zones. It is interesting that the two studies [8], [12] and this work focus on how to disperse incident-based traffic jams in two-way grid network. Long *et al.* [12] obtain a *diamond-shaped* spatial topology of traffic jam propagation and proposed a diamond control strategy which bans all vehicles entering the diamond-shaped zone. Recently, Qi *et al.* [8] use two kind signals, i.e., ban and warning signals, and cooperation with traditional traffic lights at road intersections for preventing traffic congestion caused by accidents. However, their emergency traffic light control strategies that employ warning signal lights cannot guarantee a substantial percentage of road vehicles will follow the warning signal rules. This work employs a CTM-based method to analyze the problem of traffic jams according to the number of vehicles contained in each cell. We also propose a novel traffic light TPNs control system model to implement our CTM-based control strategies.

In this study, we attempted to change the duration of the traffic light control system. We hope that our control strategies can prevent the traffic flow form heading to accident direction. Our traffic light control system consists of two phases for the traffic light duration: 1) no strategy and 2) H-strategy. The former uses a normal traffic light duration for normal conditions while H-strategy uses a traffic light duration for accidents. Traffic light control systems can regulate, alert and direct transportation to improve the safety and efficiency of pedestrians and vehicles [27]. A variety of methodologies [7]–[10], [9], [12]–[16], [27] for reducing traffic jams have been proposed. An unsuitable modeling tool can make it difficult to evaluate the performance indices of traffic control systems, such as how to decrease/increase the duration of traffic lights automatically in accident scenarios. Petri nets (PNs) have been proven to be an illuminated modeling tool for various kinds of discrete event systems (DESs) [28]–[36]. Especially, their formalism provides a clear means for presenting simulation and control logic. PNs have been successfully used to model traffic control systems as done in [26], [27] and [25], [37], [38]. Nevertheless, traditional PN lacks of the ability to determine the exact time of the transition firing. Consequently, TPNs are proposed to promote their capability [38]. Recently, TPNs have been successfully employed in grid traffic network control systems [24]–[26] and the railway level crossing traffic control work [37]. In addition, Huang *et al.* successfully employed timed colored PNs (TCPNs) to model in traffic light control systems [37], [38]. Unfortunately, existing studies do not address the issues of traffic light duration. Notably, Xu *et. al* [39] investigate the application of IoV big data in autonomous vehicles. The concept of this article can be applied to traffic congestion problems.

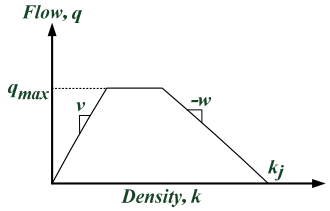

Fig. 1. The relationship of flow-density for the generalized CTM [43].

The rest of the paper is organized as follows: Section II provides the definitions of CTM and TPNs via a compact way. Section III depicts the simulation results of our traffic light control strategies. Section IV presents TPN models for our traffic light control systems. Conclusions will be explained in Section V.

II. Preliminaries

This section aims to introduce the notations of CTM [16] and describe the definitions of TPNs [26].

A. Overview of the Cell Transmission Model

To the best of our knowledge, Daganzo [11], [40] proposed the original CTM to improve the Lighthill-Whitham-Richards (LWR) model [41], [42] by adopting the following relationship between traffic flow q and density k as shown in Fig. 1:

$$q = min\{\upsilon k, q_{max}, w(k_j - k)\}, \quad 0 \leq k \leq k_j \tag{1}$$

where υ is the free flow speed and w is the speed of all backward moving waves, and q_{max} and k_j denote maximum allowable inflow and jam density, respectively.

In this study, we employ an 8×8 two-way grid network $G = (C, A)$ to demonstrate simulation results by our traffic jam control policies. C is defined as the set of nodes, A is the set of links; $a = (l, m)$ is the link formed of nodes l and m; A_l denotes the set of links heading to node l; B_m denotes the set of links leaving to node m. Here, each link is discretized into λ cells and time is partitioned into intervals such that the cell length by free-flow traffic in one time interval δ. As shown in Fig. 2, Link a is divided into two distinct zones [16]: a downstream queue storage area where vehicles are organized according to their turning movements, and an upstream reservoir where the turning movements are mixed. For a particular cell, i.e., 9^{th} cell, the downstream queue storage area consists of three divisions, i.e., q_L, q_S and q_R, which form the segregated queuing areas. Table I shows the notations that are primarily taken from Long *et al.* [16].

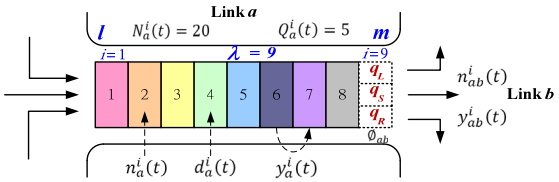

Fig. 2. Components of link a in two-way grid network.

TABLE I
NOTATIONS AND THEIR MEANINGS

Notations	Meaning
$n^i{}_a(t)$	The number of vehicles contained in cell i of link a at the start of time interval t.
$y^i{}_a(t)$	The number of vehicles that flow into cell i of link a in time interval t.
$N^i{}_a(t)$	The maximum number of vehicles that can be present in cell i of link a in time interval t.
$Q^i{}_a(t)$	The maximum number of vehicles that can flow into cell i of link a in time interval t.
$n^i{}_{ab}(t)$	The number of vehicles contained in cell i of link a and take link b as the next link at the start of time interval t.
$y^i{}_{ab}(t)$	The number of vehicles that flow into cell i of link a and take link b as the next link in time interval t.
$d^i{}_a(t)$	The sum of the congestion delay of vehicles contained in cell i of link a at time interval t.
$\emptyset_{ab}$	Proportion of vehicles traveling from link a to link b.
$d(t)$	The total congestion delay of vehicles contained in the whole network at time interval t.

For convenience, we introduce CTM [16] by a compact way. The details of the CTM will be described as follows.

$$y_i(t) = \min\{n_{i-1}(t), Q_i(t), w(N_i(t) - n_i(t))/v\} \quad (2)$$

$$n_i(t+1) = n_i(t) + y_i(t) - y_{i+1}(t) \quad (3)$$

where $y_i(t)$ is the number of vehicles that flow into cell i during time interval t, $n_i(t)$ is the number of vehicles in cell i before t, $N_i(t)$ denotes the maximum number of vehicles that can be contained in cell i during t, and $Q_i(t)$ denotes the inflow capacity in cell i during t.

Here, the inflow formulation can be classified into three categories: inflow of upstream reservoir ($i = 1$), inflow of upstream cells ($1 < i \leq 8$), and inflow of channelized downstream queue area ($i = \lambda$). We consider the influence of traffic flow lane changing behavior to illustrate the designed traffic light strategy. The inflow formulation is presented as follows:

1) Inflow of Upstream Cells: Inflow of upstream cells can be calculated by:

$$y_a^i(t) = \min\{n_a^{i-1}(t), \mathrm{Q}_a^i(t), w(N_a^i(t) - n_a^i(t)\}v, \quad 1 < i \leq 8 \quad (4)$$

From Eq. (4), we have

$$y_{ab}^i(t) = \emptyset_{ab} y_a^i(t), \quad i = 9 \quad (5)$$

2) Inflow of the Channelized Downstream Queue Area: Here, we employ the definition of $\tilde{y}_{ab}(t)$ as the up bound of inflow of the downstream queues area for vehicles travelling from link a to link b. Hence,

$$\tilde{y}_{ab}(t) = \min\{\emptyset_{ab}\mathrm{Q}_a^i(t), w(\emptyset_{ab}N_a^i(t) - n_{ab}^\lambda(t))/v\} \quad (6)$$

Because of interference between turning vehicles and ahead vehicles, the total inflow of channelized queues area can be formulated as follows.

$$y_a^\lambda(t) = \min_{b \in B_m}\{\tilde{y}_{ab}(t)/\emptyset_{ab}\} \quad (7)$$

Here, let ϕ'_{ab} denote the proportion of vehicles traveling from link a to link b (i.e., link 159 to link 161). When a ban/warning signal is displayed for direction a, direction $d$or c can be considered as the direction in which the vehicle can select the right/left turn. We have

$$\phi'_{ab} = \phi_{ab}(1 - d_x), \quad \phi'_{ac} = \phi_{ac} + \phi_{ab}(d_x/2),$$

and

$$\phi'_{ad} = \phi_{ac} + \phi_{ab}(d_x/2), \quad \text{where } x \in \{a, b, c\} \quad (8)$$

The total inflow of the channelized queues area can be obtained via Eqs. (4)-(7), where $\phi_{ab} = \phi'_{ab}$ is computed by Eq. (8).

Inflow of each direction can be calculated by Eq. (9), gives

$$y_{ab}^\lambda(t) = \min\{\emptyset_{ab} y_a^\lambda(t), \phi'_{ab} n_a^{\lambda-1}(t)\} \quad (9)$$

Hence, the update of the number of vehicles contained in each cell is formulated as follows.

$$n_a^i(t+1) = n_a^i(t) + y_a^i(t) - y_a^{i+1}(t), \quad 1 \leq i \leq \lambda \quad (10)$$

B. Basic Concepts of Timed Petri Nets [26]

A Petri net is a particular kind of bipartite directed graphs populated by three types of objects. They are places, transitions, and directed arcs connecting places to transitions and transitions to places. However, traditional Petri nets do not provide any mechanism for dealing with the duration of system activities. For solving this important issue, TPNs define the semantics that can clearly define network behavior because they are both logical and quantitative models. In TPNs, each transition, place, and/or directed arc can be associated with deterministic firing time or time interval. In this article, TPNs have their time delays associated with transitions. Note that they have the following types of transitions: 1) immediate one that is represented by a thick black bar and its firing takes no time; and 2) deterministic one that is represented by thick empty bars and its firing takes a constant delay. Formally, we have [26]:

TPN $= (P, T, I, O, H, \tau, E, M_0)$, where:

$P = \{p_1, p_2, \ldots, p_m\}$	a finite set of places that can be marked with tokens.
$T = T_{imm} \cup T_{exp} \cup T_{det}$ $= \{t_1, t_2, \ldots, t_n\}$	a finite set of transitions, partitioned into three disjoint sets, T_{imm}, T_{exp} and T_{det}, representing immediate, exponential, and deterministic ones, respectively. $P \cup T \neq 0$, and $P \cap T = 0$.

I: $P \times T \rightarrow N$	is the input function that defines directed arcs from places to transitions where $N = \{0, 1, 2, \ldots\}$.
O: $P \times T \rightarrow N$	is the output function that defines directed arcs from transitions to places.
H $\subseteq$ P $\times$ T	a set of inhibitor arcs from p to t.
$\tau : T \rightarrow R^+$	firing time function, where R^+ is a set of non-negative real numbers.
$E = \{E_1, E_2, \ldots, E_i\}$	*is a set of events associated with the transitions.*
M_0: $P \rightarrow N$	is an initial marking.

Enabling Rule: A transition t is enabled at marking M if $\forall p \in P$, $M(p) \geq I(p, t)$ and $M(p) = 0$ if $(p, t) \in H$.

Firing Rule: For one thing, an enabled transition t may or may not fire depending on the additional interpretation. For another thing, firing t removes $I(p, t)$ tokens from each input place p and deposits $O(p, t)$ tokens to each output place p of t. The liveness of a PN means that, for each marking $M \in R(M_0)$ that is reachable from M_0, it is finally possible to fire$t \forall t \in T$ through some firing sequence. Note that $R(M_0)$ is the set of all reachable markings from M_0. A marking M is reachable from M_0 if there is a fireable transition sequence that converts M_0 into M. A PN is said to be reversible if, for each marking $M \in R(M_0)$, M_0 is reachable from M. Thus, in a reversible net, it is always possible to go back to the initial marking (state) M_0.

Since TPNs allow immediate (T_{imm}), deterministic (T_{det}) and exponentially (T_{exp}) transitions, they are well suited for the modeling of real time systems in which events may occur at unknown instants. Here, each transition t is attached with a fixed enabling time duration $\tau(t)$. If t becomes enabled, then it fires after time duration $\tau(t)$. If $\tau(t) \neq 0$, t is called a deterministic transition. If $\tau(t) = 0$, t is called an immediate transition and fires at the moment when it becomes enabled. People cannot predict when an accident will occur. In this situation, we employ TPNs to model an indefinite accident event. Using this model, we can easily reproduce urgent spectacle system behaviors in the event of an accident. In this article, immediate transition has the highest priority to fire. Our control policy focuses on how to prevent traffic jams from forming due to the occurrence of accident spectacles.

III. Simulation of Traffic Jam Propagating and Dissipating

This section describes how to design a TPN model for a traffic light control system based on a CTM-based control strategy. We employ the MATLAB platform to design a traffic simulation environment for traffic jam propagation and dispersion using a time-step method. The simulation environment is based on CTM and can capture realistic traffic dynamics in detail. For convenience, we construct a two-way 8×8 grid traffic network (i.e., Fig. 3) to demonstrate traffic jam propagation while an accident is happening and how the traffic

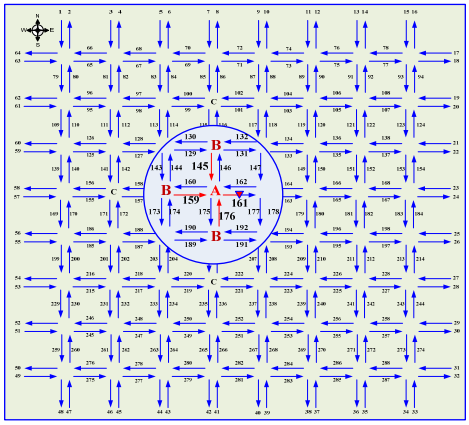

Fig. 3. A two-way 8×8 grid traffic network.

jam is dispersed while our control policy is active. The position of the inverted triangle indicates that an accident occurs in link 161. Figure 3 consists of 288 links; each link is discretised into 9 cells and each link is divided into two distinct zones: an upstream and a downstream areas. According to the results in [16], the congestion time is reduced when the channelized downstream queue area is very short. Consequently, we assume that the upstream reservoir is composed of eight cells (i.e. $i = 1, \ldots, 8$) and the channelized queue area is composed of only one cell (i.e. $i = 9$).

Fig. 2 can help us to understand the above definitions. Moreover, we define the proportions of vehicles turning left (ϕ_L), straight (ϕ_S), and right (ϕ_R) are 20%, 50% and 30%, respectively. All boundary nodes are both origins and destinations. It is worth mentioning that vehicles in the downstream queue areas will not change lanes. The inflow formulation can be classified into three categories: inflow of upstream reservoir ($i = 1$), inflow of upstream cells ($1 < i \leq \lambda - 1$), and inflow of channelized downstream queue area ($i = \lambda$). We consider the impact of traffic lane change behaviour to illustrate the design of traffic light strategies.

For convenience, the parameters for the extended CTM are set as the same as [8] and [16]. They are shown below:

1) The length of each time interval $\delta = 5s$;
2) Jam density: 133 *vehicles/km* (i.e., 7.5 m for every vehicle);
3) Free-flow speed: 54 *km/h* (i.e., 15 m/s), and backward shock-wave speed [8]: 21.6 *km/h* (i.e. 6 m/s);
4) Number of lanes: 2;
5) Flow capacity: 1800 *vehicles/h/lane*;
6) The length of each cell is 75 m, and the holding capacity of each cell is 20 vehicles;
7) The number of cells of each link: 9 (i.e. the length of every link is 675 m);
8) We define the concept of a jammed cell which can occur if the density of a cell in the upstream 'reservoir' is greater than $0.9N$; or if
9) the density of a cell in any direction of the downstream channelized area is greater than $0.9k_j$;

We assume that the initial state of the two-way 8×8 grid traffic network is empty. The analysis period of interest is

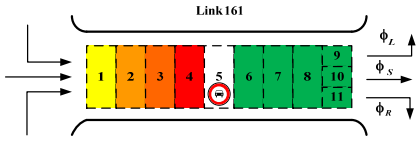

Fig. 4. An accident on the 5^{th} cell of link 161.

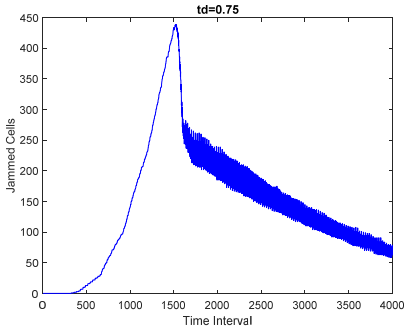

Fig. 5. All traffic jammed cells in case I.

divided into 4000 time intervals. In this study, we position an accident on the 5^{th} cell of link 161, which is located in the central zone of the network. A cell is called a jammed one if its density in the upstream reservoir or in any direction of the downstream channelized area is greater than $0.9N$ [35]. Note that the flow proportion are $\phi_L = 20\%$, $\phi_S = 50\%$ and $\phi_R = 30\%$ for all directions [16]. The downstream channelized area, i.e., the 9^{th} cell of each link, is divided into three cells 9^{th}, 10^{th} and 11^{th} for ϕ_L, ϕ_S, and ϕ_R, respectively. Figure 4 shows that an accident on the 5^{th} cell of link 161. Our simulation employs different traffic flows and is evaluated based on $t_d = 0.75$ and $t_d = 0.8$. Here, t_d is defined as the number of vehicles per time interval. For example, $t_d = 0.75$, meaning that three vehicles enter each entrance every 20 seconds. The simulation results will be described in detail in the next paragraph.

Case I (Traffic Jam Propagation): To facilitate the observation of traffic jam propagation, we assume that the accident occurs at the 301^{st} time interval and it is cleared at the 1500^{th} time interval. In this case, i.e., $t_d = 0.75$, the simulation results of traffic jam formulation and dispersion are shown in Fig. 5. We can obtain the maximal of jammed cell is 439 at 1514^{th} time interval.

A total of 335 jammed cells are formed from the beginning time interval to the 1374^{th} time interval. The distribution of the jammed cells in a two-way grid network is shown in Fig. 6. It is worth mentioning that this spatial topology of traffic jam propagation is very similar to Long *et al.* [12]. Considering the problems of traffic jam dispersion, Qi *et al.* [8] proposed a two-level strategy for preventing accident-based urban traffic congestion. In this article, the two-level strategy is called Q-strategy. Their first-level one is a ban signal strategy and the second-level one is a warning signal strategy. The former is used to stop the traffic flow heading toward an accident, the latter gives traffic flow a recommendation of not driving to the accident direction. They assume that when a ban signal is displayed for a special direction, d_A percent of vehicles headed in that direction will change their routes when a warning signal

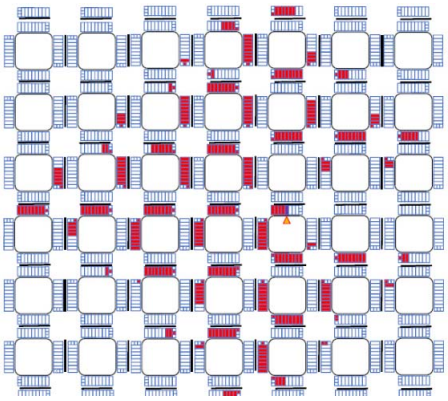

Fig. 6. Propagation of queues for an accident-based traffic jam in two-way 8×8 grid network.

is displayed, d_B percent will do so. However, the final decision for each vehicle cannot be predicted. This raises the question of how to determine the values of d_A and d_B. This question is difficult to answer in a real world situation.

Consequently, we propose a novel control strategy, called *H-strategy*, that only uses ban signals, i.e., $d_A = 1$, in intersections adjacent to prevent traffic flow in the accident direction. It hints ban signals are directly replaced by traditional red traffic lights in*H-strategy*. This paper presents a variable traffic light control system that can automatically adjust the phase duration of traffic lights when an accident occurs. We employ TPNs to design the *H-strategy* model. In this study, no strategy (i.e. no accident, with normal traffic light duration) and H-strategy (using the duration of accident traffic lights) are applied.

Case II (Traffic Jam Dispersion): For convenience, we use the same parameters as Qi *et al.* [8] in our simulation environment. They constructed a ban signal strategy that works at intersection A while the warning signal strategy works at intersection B. However, we only use ban signals in adjacent intersections, i.e., intersections$A$, B and C, to stop the traffic flow heading toward an accident. In this study, we employ d_A, d_B and d_C to represent the percent of vehicles headed in that direction will change their routes at the intersections A, B and C, *respectively*.

Example 1: We use three strategies, namely no strategy, Q-strategy and H-strategy, to observe the formation and dispersion of traffic jams. In this example, an accident occurs from the 301^{st} time interval to the 1500^{th} time interval. Here, $d_A = 1.0$ with $d_B = 0.6$; 0.8; 1.0 are for *Q-strategy* and $d_A = 1$; $d_B = 1$; $d_C = 1$ are for *H-strategy*. Two cases simulation results are shown in Figs. 7 (a) and 7(b), $t_d = 0.75$ and $t_d = 0.8$, respectively. In Fig. 7(a), i.e., with no strategy, the traffic jam begins at the 325^{th} time interval, the maximum number of jammed cells is 439 at the 1524^{th} time interval, and traffic jam dispersion takes 4000 time intervals. On the other hand, i.e., in Fig. 7(b), the traffic jam begins at the 324^{th} time interval and the maximum number of jammed cells is 506 at the 1524^{th} time interval.

According to the simulation results, the performance of traffic jam dispersion under $d_A = d_B = 1.0$ is better than that for the other two conditions ($d_A = 1.0$ with $d_B = 0.6$; 0.8).

TABLE II

JAMED CELLS NUMBER AND ITS TIME INTERVAL INFORMATION FOR EXAMPLE 1

Time interval	500	2000	4000	500	2000	4000
Strategy	T_d = 0.75 (i.e. Fig. 7 (a))			T_d = 0.8 (i.e. Fig. 7 (b))		
No strategy	13	217	63	14	265	128
d_A =1; d_B =0.6	8	120	21	8	170	72
d_A =1; d_B =0.8	7	92	12	9	147	56
d_A =1; d_B =1	10	48	0	10	87	15
H-strategy	13	36	0	14	73	6

TABLE III

JAMED CELLS NUMBER AND ITS TIME INTERVAL INFORMATION FOR EXAMPLE 2

Time interval	500	2000	4000	500	2000	4000
Strategy	T_d = 0.75 (i.e. Fig. 8 (a))			T_d = 0.8 (i.e. Fig. 8 (b))		
No strategy	13	217	63	14	265	128
H_A	8	171	42	8	215	95
H_{A+B}	10	48	0	10	87	15
H_{A+B+C}	13	36	0	14	73	6

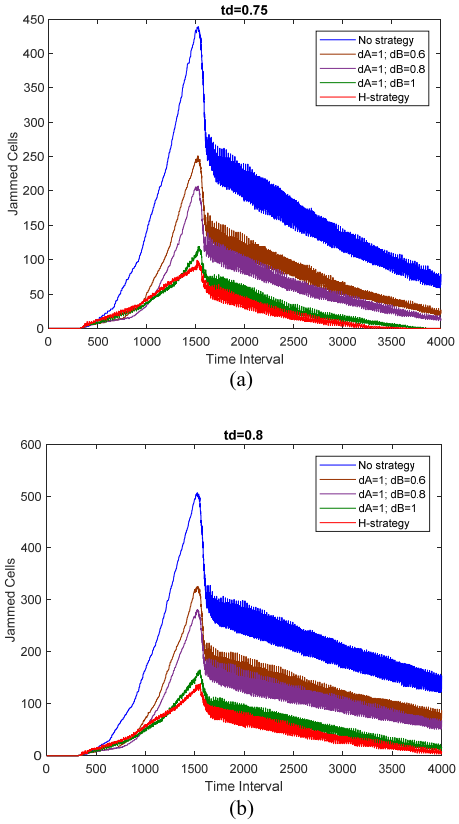

Fig. 7. (a) Traffic jam propagation and dispersion under no strategy, Q-strategy and H-strategy; $t_d = 0.75$. (b) Traffic jam propagation and dispersion under no strategy, Q-strategy and H-strategy; $t_d = 0.8$.

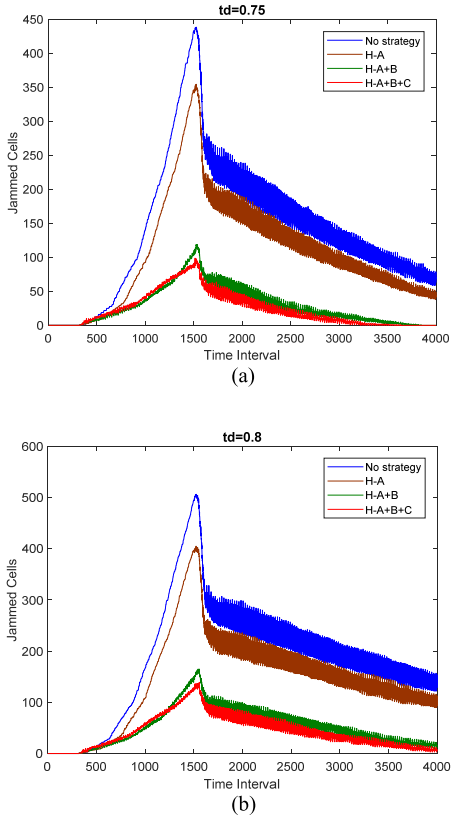

Fig. 8. (a) Traffic jam propagation and dispersion under no strategy and H-strategy; $t_d = 0.75$ and $d_A = d_B = d_C = 1.0$. (b) Traffic jam propagation and dispersion under no strategy and H-strategy; $t_d = 0.8$.

Under all strategies, dispersion takes much less time than for self-evolved traffic. In addition, Table II shows that the performance of *H-strategy* seems to be better than *Q-strategy*. Note that $d_A = d_B = d_C = 1.0$, which means that the ban signal can be regarded as a traditional red light signal.

For comparison, *H-strategy*is applied in intersection $A(d_A = 1)$, two intersections A and $B(d_A = d_B = 1)$, and three intersections A, B and $C(d_A = d_B = d_C = 1.0)$, which are called H_A, H_{A+B}, andH_{A+B+C}, respectively.

Example 2: We use four strategies, namely no strategy, H_A, H_{A+B}, and H_{A+B+C}, to observe the formation and dispersion of traffic jams to cope with the same accidents.

Two conditions $t_d = 0.75$ and $t_d = 0.8$ are applied in our simulation environment, there are four simulation results are shown in Fig. 8(a) and Fig. 8(b), respectively. In Fig. 8(a), we can know that traffic jams begin at the 325^{th} time interval under no strategy, the maximum number of jammed cell is 439 at the 1524^{th} time interval, and the traffic jam dispersion takes 4000 time intervals. According to the simulation results, the performance of traffic jam dispersion under H_{A+B+C} is better than that for the other two control strategies H_A and H_{A+B}. In Fig. 8(b), the traffic jams begin at 324^{th} time interval and the maximum number of jammed cell is 506 at the 1524^{th} time interval. According to the simulation results, the performance of traffic jam dispersion under H_{A+B+C} is also better than the other two. Under all strategies, dispersion takes much less time than self-evolved traffic. Additionally, Table III shows that among all the strategies, H_{A+B+C} is the best, regardless of the conditions for $t_d = 0.75$ and $t_d = 0.8$.

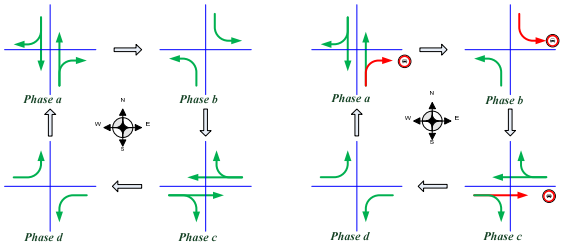

(a) No strategy. (b) *H*-strategy

Fig. 9. The phase duration of traffic light signals.

IV. Design of Traffic Light Control Systems TPNs Model

This section presents how to design a TPNs model of traffic light control systems according to our CTM-based control strategies. To do so, this section aims to describe the phase transitions of traffic lights at signalized intersections and establish the normal traffic light control strategy and *H-strategy* based on TPNs. Simply, *H-strategy* refers to the duration of using traditional traffic lights under normal conditions. Once an accident occurs, the duration of phase traffic lights changes from the normal state to the accident state. In this study, seven adjacent intersections which are one A, three B and three C are involved. As mentioned earlier, *H-strategy* only employs ban signals to stop the traffic flow heading in the direction of an accident. For convenience, all traffic lights consist of five signal lights: a left-turn arrow on green (GL), a right-turn arrow on green (GR), a straight arrow on green (GS), a yellow light signal (Y), and a red light signal(R). In this work, we adopt four-phase traffic light rules to guide traffic flow at signalized intersections, as shown in Fig. 9.

Fig. 9(a) shows a normal traffic light duration that is used for normal condition in the grid network. Fig. 9(b) shows accident traffic lights duration that is employed if an accident occurs. In this study, we assume the duration of phases a and c are 30 s and phases b and d is 20 s. It states that phase a changes to b after 30 s and phase b changes to c after 20 s. Consequently, the duration of a set period of time (i.e. phase a changing to d) is 110 s. It is worthwhile to mention that some important rules for the roadways are indispensable to the vehicle safety.

1) A traffic light control system can be started if its traffic signal lights are all in a red state,
2) There is five seconds overlap between the phases to change, for example, in this article, there is five seconds overlap between the durations of phase b/d changes to phase c/a,
3) No green lights are allowed to be on simultaneously, and
4) A traffic light changes in the order of red, green, and yellow.

For convenience, the directions of vehicles heading northward, southward, westward, and eastward are indicated by the symbols *n, s, w*and*e,*respectively. For example, R_s, Y_s, GL_s, GR_s, and GS_s, represent the five traffic lights R, Y, GL, GR, and GS for the directions of vehicles heading southward, respectively. Additionally, in this study, we assume that $\sigma \in \{n, e, s, w\}$, $\gamma \in \{s, n\}$, and $\eta \in \{w, e\}$. The detailed operations are described in Fig. 10 and modeled by TPN. The interpretation of TPN system model's transitions are listed in Table IV.

TABLE IV
Interpretation of Transitions in Fig. 10

T	Meaning	$\tau(s)$	P	Meaning
t_{ns}	phase changing	55	p_1	system ready
t_{we}	phase changing	55	p_2	phase complied
$t_{1\gamma}$	system starting	2	$p_{s(n)gr}$	$GR_{s(n)}$
$t_{1\gamma\gamma}$	normal mode	$\varepsilon\to 0^+$	$p_{s(n)gs}$	$GS_{s(n)}$
$t_{2\gamma}$	$^*GS_{s(n)}$, $GR_{s(n)}\to GL_{s(n)}$	30	$p_{s(n)gl}$	$GL_{s(n)}$
$t_{3\gamma}$	$GL_{s(n)}\to Y_{s(n)}$	20	$p_{s(n)y}$	$Y_{s(n)}$
$t_{4\gamma}$	$Y_{s(n)}\to R_{s(n)}$	3	$p_{s(n)r}$	$R_{s(n)}$
t_{ie}	accident	0	$p_{w(e)gr}$	$GR_{w(e)}$
$t_{5\eta}$	phase changing	2	$p_{w(e)gs}$	$GS_{w(e)}$
$t_{5\eta\eta}$	normal mode	$\varepsilon\to 0^+$	$p_{w(e)gl}$	$GL_{w(e)}$
$t_{6\eta}$	$GS_{w(e)}$, $GR_{w(e)}\to GL_{w(e)}$	30	$p_{w(e)y}$	$Y_{w(e)}$
$t_{7\eta}$	$GL_{w(e)}\to Y_{w(e)}$	20	$p_{w(e)r}$	$R_{w(e)}$
$t_{8\eta}$	$Y_{w(e)}\to R_{w(e)}$	3	p_3-p_6	control place
t_{iet}	accident mode	30		

$^*GS_{s(n)}$ meaning GS_s and GS_n turn on together.

Figure 10 shows H-strategy TPN models that places p_{sr}, p_{nr}, p_{wr}, and p_{er} are with one token except p_1 with three ones. It states that the initial state of traffic signal lights is in the R state. First at all, we introduce how the no strategy works. After firing both t_{1s} and t_{1n} (2 s), one token is moved to p_3 and p_4 from p_{sr} and p_{nr}, respectively. At the meantime, p_1 holds back one token. In the meantime, $t_{1ss}(t_{1nn})$ fire immediately such that a token is moved to p_{sgr}, p_{sgs}, p_{ngr}, and p_{ngs} immediately. In the meantime, $GR_{s(n)}$ and $GS_{s(n)}$ turn on such that the way of vehicles can pass through the intersection (i.e., Fig. 9(a), *phase a* processing with 30 s). Next, $GR_{s(n)}$ and $GS_{s(n)}$ should be off after the duration in $t_{2s}(t_{2n})$. At this moment, $GL_{s(n)}$ turn on such that the way of vehicles can pass through the intersection (i.e., Fig. 9(a), *phase b* processing with 20 s). After 20 s (i.e., firing $t_{3s}(t_{3n})$), a token in $p_{sgl}(p_{ngl})$ is moved to $p_{sy}(p_{ny})$. Then, a token in $p_{sy}(p_{ny})$ is moved to $p_{sr}(p_{nr})$ after 3 s. At this moment, the duration of phase $a$and b is achieved. As mentioned earlier, two seconds between the durations of phase b changes to phase c. Up to now, it spends 55 s. Next, after firing t_{we}, the one in p_1 is moved to p_2. Note that p_2 will get three tokens because the input arc of p_2 with the weight value is 3. Continually, after firing $t_{5w}(t_{5e})$, a token is moved to $p_5(p_6)$ from $p_{wr}(p_{er})$. At this meantime, p_2 holds back one token. In the meantime, $t_{5ww}(t_{5ee})$ fire immediately such that a token is moved to p_{wgr}, p_{wgs}, p_{egr}, and p_{egs} immediately. At this moment, $GR_{w(e)}$ and $GS_{w(e)}$ turn on such that the way of vehicles can pass through the intersection (i.e., Fig. 9(a), *phase c* processing with 30 s). Next, $GR_{w(e)}$ and $GS_{w(e)}$ should be off after the duration in $t_{6w}(t_{6e})$.

At this moment, $GL_{w(e)}$ turn on such that the way of vehicles can pass through the intersection (i.e., Fig. 9(a),

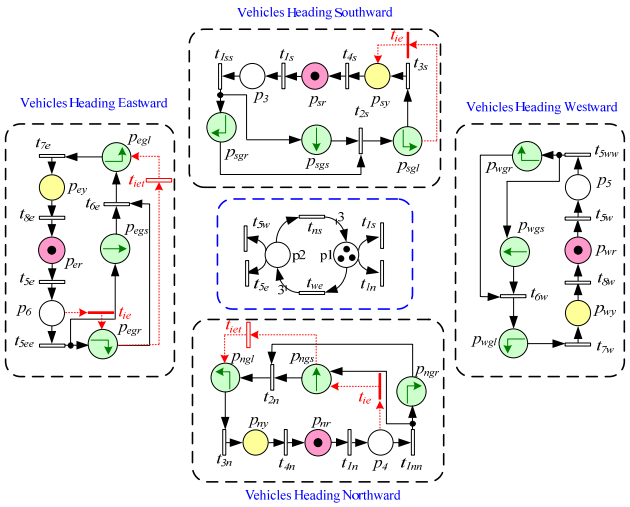

Fig. 10. TPN models of *H-strategy* at intersection A.

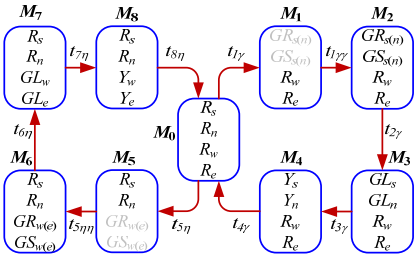

Fig. 11. No strategy reachability graph of TPN models.

phase d processing with 20 s). After 20 s (i.e., firing $t_{7w}(t_{7e})$), a token in $p_{wgl}(p_{egl})$ is moved to $p_{wy}(p_{ey})$. Next, a token in $p_{wy}(p_{ey})$ is moved to $p_{wr}(p_{er})$ after 3 s. At this moment, the duration of phase c and d is achieved. Once t_{ns} fires, TPN models return to their initial state. For a better understanding, we proposed timed reachability graph of these TPN models to analyze whether the system models are reversible or not. These TPN models firing sequence is $t_{1\gamma} \rightarrow t_{1\gamma\gamma} \rightarrow t_{2\gamma} \rightarrow t_{3\gamma} \rightarrow t_{4\gamma} \rightarrow t_{5\eta} \rightarrow t_{5\eta\eta} \rightarrow t_{6\eta} \rightarrow t_{7\eta} \rightarrow t_{8\eta}$. According to this firing sequence, we can construct their reachability graph as shown in Fig. 11. Here, M_0 states its traffic signal lights are all in a red state. M_2 shows that its traffic signal lights GS_s, GS_n, GR_s, and GR_n, are turning on. M_3 shows GL_s, GL_n,R_w, and R_e are in on. In other words, M_2/M_3 is processing the duration of phase a/b. As a result, no conflict can be found in Fig. 11 as verified by its reachability graph.

It is interesting to discuss the conflict problems in TPNs when both deterministic and immediate transitions are concurrently triggered. The immediate transition will fire first when both deterministic and immediate transitions are concurrently triggered. Note that the gray font in all reachability graphs indicates that traffic lights marked in gray fonts are disabled. For example, t_{ie} fires first if both $t_{1\gamma\gamma}$ and t_{ie} are concurrently triggered.

Here, we introduce the detailed operations of the H-strategy. For convenience, we use the notation " : " to indicate two concurrent transitions; for example, t_x:t_y means that t_x and t_y are concurrent transitions. As the same as the previously mentioned, after firing both t_{1s} and t_{1n}, one token is moved to p_3 and p_4 from p_{sr} and p_{nr}, respectively. At this moment, we assume that an accident occurs in the eastbound and upstream lanes (t_{ie} triggers) as shown in Fig. 10. It hints that t_{1ss}, t_{1nn}, and t_{ie} are enabled. A token is moved top_{sgr} and p_{sgs} from p_3 via t_{1ss} firing and a token is moved to p_{ngs} from p_4 via t_{ie} firing. It is worthy to notice that an immediate transition (t_{ie}) also has higher priority to fire than a timed one (t_{1nn}) in TPNs such that t_{1nn} cannot fire. In the meantime, GR_s and $GS_{s(n)}$ turn on such that the way of vehicles can pass through the intersection (i.e., Fig. 9(b), *phase a* processing with 30 s). Next, a token is moved to p_{sgl} by t_{2s} firing and a token is moved to p_{ngl} by t_{iet} firing. Hence, GR_s and $GS_{s(n)}$ should be off after the duration in t_{2s}:t_{iet}. At this moment, GL_n turns on only, i.e., a token is move to p_{sy} by t_{ie} immediate, such that the way of vehicles can pass through the intersection (i.e., Fig.10(b), *phase b* processing with 20 s). After 20 s (i.e., firing $t_{3s}(t_{3n})$), a token in p_{ngl} is moved to p_{ny}. Then, a token in $p_{sy}(p_{ny})$ is moved to $p_{sr}(p_{nr})$ by $t_{4s}(t_{4n})$ after 3 s. At this moment, the duration of phase $a$and b in Fig. 9(b) is achieved. Up to now, it spends 55 s. Like the previous mentioned steps, after firing t_{we}, the one token in p_1 is moved to p_2. Then, after firing $t_{5w}(t_{5e})$, a token is moved to $p_5(p_6)$ from $p_{wr}(p_{er})$. Note that the accident is not clearly at this moment. In the meantime, t_{5ww} fires immediately such that a token is moved to p_{wgr} and p_{wgs}. Note that t_{5ee} cannot fire because t_{ie} has higher priority than t_{5ee}. Consequently, a token is moved to p_{egr} from p_6. At this moment, $GR_{w(e)}$ and GS_w turn on such that the way of vehicles can pass through the intersection (i.e., Fig. 9(b), *phase c* processing with 30 s). Next, a token is moved to p_{wgl} by t_{6w} firing and a token is moved top_{egl} by t_{iet} firing. Hence, GR_e, GS_w and GR_w should be off after the duration in t_{6w}:t_{iet}. At this moment, GL_w and GL_e turn on such that the way of vehicles can pass through the intersection (i.e., Fig. 9(b), *phase d* processing with 20 s). After 20 s (i.e., firing $t_{7w}(t_{7e})$), a token in $p_{wgl}(p_{egl})$ is moved to $p_{wy}(p_{ey})$. Next, a token in $p_{wy}(p_{ey})$ is moved to $p_{wr}(p_{er})$ after 3 s. At this moment, the duration of phase c and d, i.e., Fig. 9(b), is achieved. Once t_{ns} fires, TPN models return to their initial state. For a better understanding, we introduce the detailed transitions firing sequence of the H-strategy. TPN models of H-strategy firing sequence is $t_{1\gamma} \rightarrow t_{ie} \rightarrow t_{1\text{ss}} \rightarrow t_{2\text{s}}$:$t_{iet} \rightarrow t_{ie} \rightarrow t_{4\text{s}} \rightarrow t_{3n} \rightarrow t_{4\text{n}} \rightarrow t_{5\eta} \rightarrow t_{ie} \rightarrow t_{5ww} \rightarrow t_{6\text{w}}$:$t_{iet} \rightarrow t_{7\eta} \rightarrow t_{8\eta}$. According to this firing sequence, we can construct their reachability graph as shown in Fig. 12. As a result, no conflict can be found in Fig. 12 as verified by its reachability graph. Hence, one can infer that the accident spectacle can be avoided by our traffic control system.

V. Analysis of the Whole System TPNs Model

According to the previous discussion, once an accident occurs, how to prevent vehicles from entering the location of the accident position is an important issue. In this work, we propose an extremely effective control strategy to adjust the duration of the traffic lights that depends entirely on the

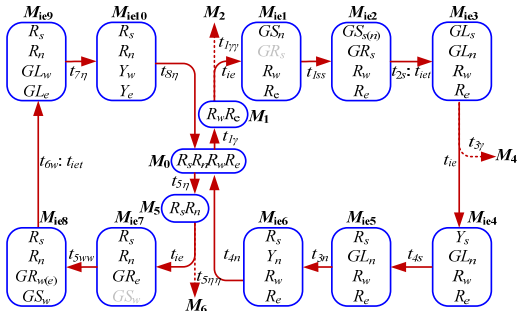

Fig. 12. H-strategy reachability graph of TPN models (t_{ie} enable).

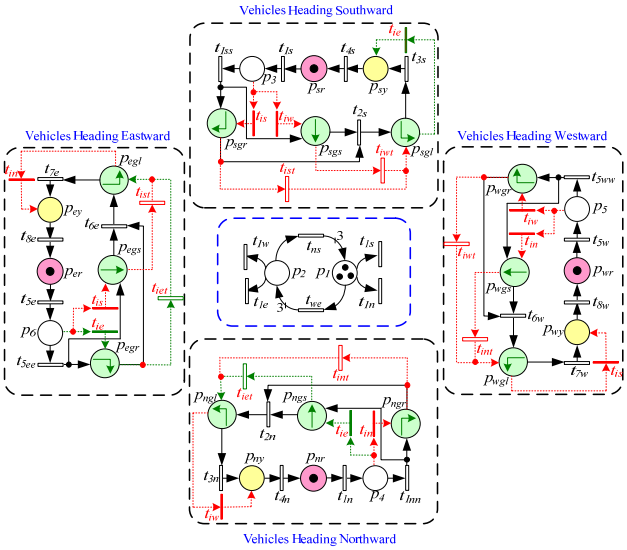

Fig. 13. The whole TPN model of *H-strategy* at intersection A.

TABLE V
INTERPRETATION OF TRANSITIONS IN FIG. 13

T	Meaning	$\tau(s)$	P	Meaning
t_{ns}	phase changing	55	p_1	system ready
t_{we}	phase changing	55	p_2	phase complied
$t_{1\gamma}$	system starting	2	$p_{s(n)gr}$	$GR_{s(n)}$
$t_{1\gamma\gamma}$	normal mode	$\varepsilon\to 0^+$	$p_{s(n)gs}$	$GS_{s(n)}$
$t_{2\gamma}$	${}^*GS_{s(n)}$, $GR_{s(n)}\to GL_{s(n)}$	30	$p_{s(n)gl}$	$GL_{s(n)}$
$t_{3\gamma}$	$GL_{s(n)}\to Y_{s(n)}$	20	$p_{s(n)y}$	$Y_{s(n)}$
$t_{4\gamma}$	$Y_{s(n)}\to R_{s(n)}$	3	$p_{s(n)r}$	$R_{s(n)}$
$t_{i\sigma}$	accident	0	$p_{w(e)gr}$	$GR_{w(e)}$
$t_{5\eta}$	phase changing	2	$p_{w(e)gs}$	$GS_{w(e)}$
$t_{5\eta\eta}$	normal mode	$\varepsilon\to 0^+$	$p_{w(e)gl}$	$GL_{w(e)}$
$t_{6\eta}$	$GS_{w(e)}$, $GR_{w(e)}\to GL_{w(e)}$	30	$p_{w(e)y}$	$Y_{w(e)}$
$t_{7\eta}$	$GL_{w(e)}\to Y_{w(e)}$	20	$p_{w(e)r}$	$R_{w(e)}$
$t_{8\eta}$	$Y_{w(e)}\to R_{w(e)}$	3	p_3-p_6	control place
$t_{i\sigma t}$	accident mode	30		

* let $\sigma\in\{n,e,s,w\}$, $\gamma\in\{s,n\}$, and $\eta\in\{w,e\}$.

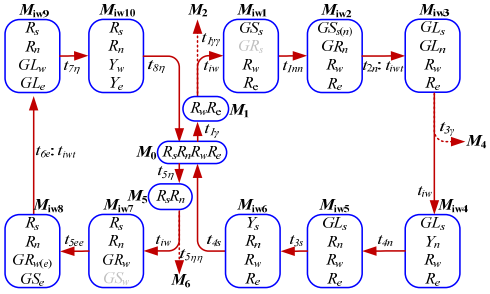

Fig. 14. The H-strategy reachability graph of TPN models (t_{iw} enable).

location of the accident. To do so, we add three transitions t_{iwt}, t_{int}, and t_{ist} on the TPN model of *H-strategy*, i.e. called the whole TPN system model and shown in Fig. 13, to trigger an accident occurs in either direction of vehicles heading westward, northward or southward, respectively. The interpretation of transitions is listed in Table V. Here, four cases are given to illustrate the whole TPN system model how to work well.

Case I (No Control Strategy): In this case, a firing sequence $t_{1\gamma}\to t_{1\gamma\gamma}\to t_{2\gamma}\to t_{3\gamma}\to t_{4\gamma}\to t_{5\eta}\to t_{5\eta\eta}\to t_{6\eta}\to t_{7\eta}\to t_{8\eta}$ is for normal conditions. According to the firing sequence, we can construct the corresponding reachability graph of the firing sequence is as shown in Fig. 17. It states the whole TPN system model in normal mode is live and reversible.

Case II (H-Strategy for an Accident in the Direction of the West): In this case, one can understand that how a phase duration of traffic light will be altered by an accident. For example, once an accident occurs in the direction for vehicles heading westward, t_{iw} fires immediately.

Therefore, we can obtain that the whole TPN models of H-strategy firing sequence is $t_{1\gamma}\to t_{iw}\to t_{1nn}\to t_{2n}{:}t_{iwt}\to t_{iw}\to t_{4n}\to t_{3s}\to t_{4s}\to t_{5\eta}\to t_{iw}\to t_{5ee}\to t_{6e}{:}t_{iwt}\to t_{7\eta}\to t_{8\eta}$. According to the firing sequence, one can depict the corresponding reachability graph (i.e. t_{iw} enable) of the firing sequence is as shown in Fig. 14. One can know that the whole TPN system model in this case is live and reversible.

Case III (H-Strategy for an Accident in the Direction of the North): In this case, once an accident occurs in the direction of vehicles heading northward, t_{in} fires immediately. By the same way, one can describe the corresponding reachability graph (i.e. t_{in} enable) of the firing sequence is as shown in Fig. 15. Here, one can find that the trace of the reachability graph is $M_0 t_{in} M_{in1} t_{1ss}\ M_{in2} t_{2s}{:}t_{int} M_{in3} t_{3\gamma} M_{in4} t_{4\gamma} M_0 t_{5\eta} M_5 t_{in} M_{in5} t_{5ee} M_{in6} t_{6e}{:}t_{int} M_{in7} t_{in} M_{in8} t_{8e} M_{in9} t_{7w} M_{in10} t_{8w} M_0$. One can infer that that the whole TPN system model in this case is live and reversible.

Case IV (H-Strategy for an Accident in the Direction of the South): In this case, once an accident occurs in the directions of vehicles heading southward, t_{is} fires immediately. By the same way, one can create the corresponding reachability graph (i.e. t_{is}enable) of the firing sequence is as shown in Fig. 16. Here, one can find that the trace of the reachability graph is $M_0\ t_{is}\ M_{is1}\ t_{1nn}\ M_{is2}\ t_{2n}{:}t_{ist}\ M_{is3}\ t_{3\gamma}\ M_{is4}\ t_{4\gamma}\ M_0\ t_{5\eta}\ M_5 t_{is}\ M_{is5}\ t_{5ww}\ M_{is6}\ t_{6w}{:}t_{ist}\ M_{is7} t_{is}\ M_{is8} t_{8w}\ M_{is9}\ t_{7e}\ M_{is10}\ t_{8e}\ M_0$. Note that all heading southward traffic signals

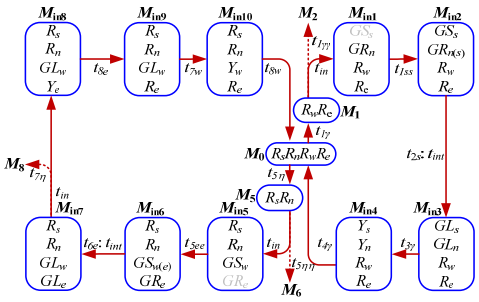

Fig. 15. H-strategy reachability graph of TPN models (t_{in} enable).

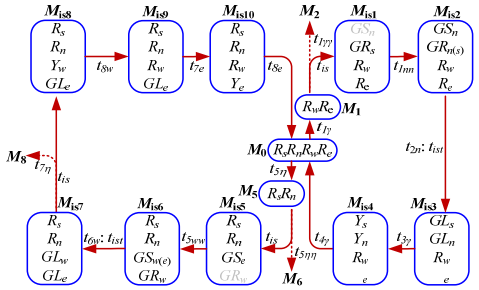

Fig. 16. H-strategy reachability graph of TPN models (t_{is} enable).

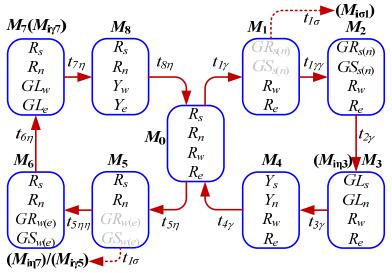

Fig. 17. H-strategy reachability graph of TPN whole models ($t_{i\sigma}$ enable).

are terminated. One can know that that the whole TPN system model in case IV is live and reversible.

In the real world, no one knows when an accident will happen. However, we know that immediate transition has the highest priority to fire. We use its inherent characteristics to model our TPN traffic light control system model. Note that transitions t_{iet}, t_{iwt}, t_{int}, and t_{ist} are employed to maintain the consistency of the phase duration of traffic lights when an accident occurs somewhere. On the other hand $t_{1\gamma\gamma}$ and $t_{5\eta\eta}$ are used to describe how to resume normal operations (normal mode) when the accident is removed. It hints that our TPN traffic light control system model can use in a real world situation. Consequently, we can conclude that our TPN traffic light control system model is live and reversible.

VI. Conclusion

In this article, the MATLAB platform is used to design a traffic simulation tool based on CTM, which successfully simulates the propagation and dispersion of traffic congestion caused by an accident. In order to effectively disperse the traffic congestion caused by an accident, an extremely effective control strategy, called *H-strategy*, to adjust the duration of traffic lights that depends entirely on the location of the accident is presented. More importantly, *H-strategy* only uses traditional traffic lights in intersections adjacent to the accident site at the scene of the accident to prevent traffic from flowing to the direction of the accident. This work has demonstrated how to use TPNs to model *H-strategy* traffic light control systems, verify the liveness and reversibility of the proposed TPN models and the problem of traffic jam from the models and ways to avoid them. The liveness and reversibility of the proposed TPN models are proven by the reachability graph analysis method. The advantage of the proposed approach is that traffic jams in the traffic light control system can be identified and avoided based on conditions and events in the system model that cause alternations in the traffic lights phase. The proposed *H-strategy* traffic light control systems and its TPN models should be extended for their further applications.

References

[1] B. M. Williams and A. Guin, "Traffic management center use of incident detection algorithms: Findings of a nationwide survey," *IEEE Trans. Intell. Transp. Syst.*, vol. 8, no. 2, pp. 351–358, Jun. 2007.

[2] S. Chen, W. Wang, and H. V. Zuylen, "Construct support vector machine ensemble to detect traffic incident," *Expert Syst. Appl.*, vol. 36, no. 8, pp. 10976–10986, Oct. 2009.

[3] B. A. Coifman and R. Mallika, "Distributed surveillance on freeways emphasizing incident detection and verification," *Transp. Res. A, Policy Pract.*, vol. 41, no. 8, pp. 750–767, Oct. 2007.

[4] K. G. Zografos, K. N. Androutsopoulos, and G. M. Vasilakis, "A real-time decision support system for roadway network incident response logistics," *Transp. Res. C, Emerg. Technol.*, vol. 10, no. 1, pp. 1–18, 2002.

[5] R. N. Mussa and J. E. Upchurch, "Monitoring urban freeway incidents by wireless communications," *Transp. Res. Rec., J. Transp. Res. Board*, vol. 1748, no. 1, pp. 153–160, Jan. 2001.

[6] L. Figueiredo, J. A. T. Machado, and J. R. Ferreira, "Dynamical analysis of freeway traffic," *IEEE Trans. Intell. Transp. Syst.*, vol. 5, no. 4, pp. 259–266, Dec. 2004.

[7] C. Wright and P. Roberg, "The conceptual structure of traffic jams," *Transp. Policy*, vol. 5, no. 1, pp. 23–35, 1998.

[8] L. Qi, M. Zhou, and W. Luan, "A two-level traffic light control strategy for preventing incident-based urban traffic congestion," *IEEE Trans. Intell. Transp. Syst.*, vol. 19, no. 1, pp. 13–24, Jan. 2018.

[9] P. Roberg, "A distributed strategy for eliminating incident-based traffic jams from urban networks," *Traffic Eng. Control*, vol. 36, no. 6, pp. 348–355, 1995.

[10] P. Roberg-Orenstein, C. R. Abbess, and C. Wright, "Traffic jam simulation," *J. Maps*, vol. 3, no. 1, pp. 107–121, 2007.

[11] C. F. Daganzo, "The cell transmission model: A dynamic representation of highway traffic consistent with the hydrodynamic theory," *Transp. Res. B, Methodol.*, vol. 28, no. 4, pp. 269–287, 1994.

[12] J. Long, Z. Gao, P. Orenstein, and H. Ren, "Control strategies for dispersing incident-based traffic jams in two-way grid networks," *IEEE Trans. Intell. Transp. Syst.*, vol. 13, no. 2, pp. 469–481, Jun. 2012.

[13] P. Roberg, "The development and dispersal of area-wide traffic jams," *Traffic Eng. Control*, vol. 35, no. 6, pp. 379–386, Jun. 1994.

[14] P. Roberg and C. R. Abbess, "Diagnosis and treatment of congestion in central urban areas," *Eur. J. Oper. Res.*, vol. 104, no. 1, pp. 218–230, Jan. 1998.

[15] C. Wright and P. Roberg-Orenstein, "Simple models for traffic jams and congestion control," *Proc. Inst. Civil Eng., Transp.*, vol. 135, no. 3, pp. 123–130, 1999.

[16] J. Long, Z. Gao, X. Zhao, A. Lian, and P. Orenstein, "Urban traffic jam simulation based on the cell transmission model," *Netw. Spatial Econ.*, vol. 11, no. 1, pp. 43–64, Mar. 2011.

[17] L. Li, Y. Lv, and F.-Y. Wang, "Traffic signal timing via deep reinforcement learning," *IEEE/CAA J. Automat. Sinica*, vol. 3, no. 3, pp. 247–254, Apr. 2016.

[18] S. F. Cheng, M. A. Epelman, and R. L. Smith, "CoSIGN: A parallel algorithm for coordinated traffic signal control," *IEEE Trans. Intell. Transp. Syst.*, vol. 7, no. 4, pp. 551–564, Dec. 2006.

[19] B. D. Schutter and B. D. Moor, "Optimal traffic light control for a single intersection," *Eur. J. Control*, vol. 4, no. 3, pp. 260–276, 1998.

[20] N. Geroliminis, J. Haddad, and M. Ramezani, "Optimal perimeter control for two urban regions with macroscopic fundamental diagrams: A model predictive approach," *IEEE Trans. Intell. Transp. Syst.*, vol. 14, no. 1, pp. 348–359, Mar. 2013.

[21] K. Aboudolas, M. Papageorgiou, A. Kouvelas, and E. Kosmatopoulos, "A rolling-horizon quadratic-programming approach to the signal control problem in large-scale congested urban road networks," *Transp. Res. C, Emerg. Technol.*, vol. 18, no. 5, pp. 680–694, Oct. 2010.

[22] A. Kouvelas, K. Aboudolas, M. Papageorgiou, and E. B. Kosmatopoulos, "A hybrid strategy for real-time traffic signal control of urban road networks," *IEEE Trans. Intell. Transp. Syst.*, vol. 12, no. 3, pp. 884–894, Sep. 2011.

[23] S. Zhao, Y. Chen, and J. A. Farrell, "High-precision vehicle navigation in urban environments using an MEM's IMU and single-frequency GPS receiver," *IEEE Trans. Intell. Transp. Syst.*, vol. 17, no. 10, pp. 2854–2867, Oct. 2016.

[24] Y.-S. Huang and P.-J. Su, "Modelling and analysis of traffic light control systems," *IET Control Theory Appl.*, vol. 3, no. 3, pp. 340–350, Mar. 2009.

[25] L. Qi, M. Zhou, and Z. Ding, "Real-time traffic camera-light control systems for intersections subject to accidents: A Petri net approach," in *Proc. IEEE Int. Conf. Syst., Man, Cybern.*, Manchester, U.K., Oct. 2013, pp. 1069–1074.

[26] Y.-S. Huang, Y.-S. Weng, and M. Zhou, "Modular design of urban traffic-light control systems based on synchronized timed Petri nets," *IEEE Trans. Intell. Transp. Syst.*, vol. 15, no. 2, pp. 530–539, Apr. 2014.

[27] Y.-S. Huang, Y.-S. Weng, W. Wu, and B.-Y. Chen, "Control strategies for solving the problem of traffic congestion," *IET Intell. Transp. Syst.*, vol. 10, no. 10, pp. 642–648, Dec. 2016.

[28] B. Huang, M. Zhou, Y. Huang, and Y. Yang, "Supervisor synthesis for FMS based on critical activity places," *IEEE Trans. Syst., Man, Cybern., Syst.*, vol. 49, no. 5, pp. 881–890, May 2019.

[29] B. Huang, M. Zhou, P. Zhang, and J. Yang, "Speedup techniques for multiobjective integer programs in designing optimal and structurally simple supervisors of AMS," *IEEE Trans. Syst., Man, Cybern. Syst.*, vol. 48, no. 1, pp. 77–88, Jan. 2018.

[30] Y. Wang *et al.*, "Multi-objective workflow scheduling with deep-Q-network-based multi-agent reinforcement learning," *IEEE Access*, vol. 7, pp. 39974–39982, 2019. doi: 10.1109/ACCESS.2019.2902846.

[31] Q. Peng, M. Zhou, Q. He, Y. Xia, C. Wu, and S. Deng, "Multi-objective optimization for location prediction of mobile devices in sensor-based applications," *IEEE Access*, vol. 6, pp. 77123–77132, 2018.

[32] W. Li, Y. Xia, M. Zhou, X. Sun, and Q. Zhu, "Fluctuation-aware and predictive workflow scheduling in cost-effective infrastructure-as-a-service clouds," *IEEE Access*, vol. 6, pp. 61488–61502, 2018.

[33] C. Pan, M. Zhou, Y. Qiao, and N. Wu, "Scheduling cluster tools in semiconductor manufacturing: Recent advances and challenges," *IEEE Trans. Autom. Sci. Eng.*, vol. 15, no. 2, pp. 586–601, Apr. 2018.

[34] C. Pan, Y. Qiao, N. Wu, and M. Zhou, "A novel algorithm for wafer sojourn time analysis of single-arm cluster tools with wafer residency time constraints and activity time variation," *IEEE Trans. Syst., Man, Cybern. Syst.*, vol. 45, no. 5, pp. 805–818, May 2015.

[35] G. Cavone, M. Dotoli, and C. Seatzu, "A survey on Petri net models for freight logistics and transportation systems," *IEEE Trans. Intell. Transp. Syst.*, vol. 19, no. 6, pp. 1795–1813, Jun. 2018.

[36] Z. He, Z. W. Li, and A. Giua, "Performance optimization for timed weighted marked graphs under infinite server semantics," *IEEE Trans. Autom. Control*, vol. 63, no. 8, pp. 2573–2580, Aug. 2018.

[37] Y.-S. Huang, Y.-S. Weng, and M. Zhou, "Critical scenarios and their identification in parallel railroad level crossing traffic control systems," *IEEE Trans. Intell. Transp. Syst.*, vol. 11, no. 4, pp. 968–977, Dec. 2010.

[38] Y.-S. Huang and T.-H. Chung, "Modeling and analysis of urban traffic light control systems," *J. Chin. Inst. Eng.*, vol. 32, no. 1, pp. 85–95, 2009.

[39] W. Xu *et al.*, "Internet of vehicles in big data era," *IEEE/CAA J. Autom. Sinica*, vol. 5, no. 1, pp. 19–35, Jan. 2018.

[40] C. F. Daganzo, "The cell transmission model, part II: Network traffic," *Transp. Res. B, Methodol.*, vol. 29, no. 2, pp. 79–93, 1995.

[41] M. J. Lighthill and G. B. Whitham, "On kinematic waves. II. A theory of traffic flow on long crowded roads," *Proc. Roy. Soc. London, Ser. A, Math. Phys. Sci.*, vol. 229, no. 1178, pp. 317–345, 1955.

[42] P. I. Richards, "Shock waves on the highway," *Oper. Res.*, vol. 4, no. 1, pp. 42–51, 1956.

[43] J. Haddad and N. Gerolimins, "On the stability of traffic perimeter control in two-region urban cities," *Transp. Res. B, Methodol.*, vol. 46, no. 1, pp. 1159–1176, 2012.

Jiliang Luo received the B.S. and M.S. degrees in thermal power engineering from Northeast Dianli University, Jilin, China, in 2000 and 2003, respectively, and the Ph.D. degree in control science and engineering from Zhejiang University, Hangzhou, China, in 2006. He joined Huaqiao University, Xiamen, China, in 2006. He was a Visiting Researcher at Chiba University from 2009 to 2010, and also at the New Jersey Institute of Technology from 2014 to 2015. He is currently a Professor with the College of Information Science and Engineering, Huaqiao University, and also with the Fujian Engineering Research Center of Motor Control and System Optimal Schedule, Xiamen. His research interests are in supervisory control of discrete event systems, Petri nets, programmable logic controllers (PLC), intelligent manufacturing systems, and robots. He was a recipient of the Ho-Pan-Qing-Qi Award of 2012 and the ASIAN JOURNAL OF CONTROL's Outstanding Reviewer of 2011.

Yi-Sheng Huang (M'01–SM'07) received the B.S. degree in automatic control engineering from Feng Chia University, Taiwan, in 1989, the M.S. degree in electronic engineering from Chung Yuan Christian University, Taiwan, in 1991, and the Ph.D. degree in electrical engineering from the National Taiwan University of Science and Technology (NTUST), Taiwan, in 2001.

He was a Professor at the Department of Electrical and Electronic, Chung Cheng Institute of Technology (CCIT), National Defense University, Taiwan. He was a Visiting Professor with the Department of Electrical and Computer Engineering, New Jersey Institute of Technology, Newark, NJ, USA, in 2008 and 2014, respectively. He is currently a Professor and the Chairman of the Department of Electrical Engineering, National Ilan University, Taiwan. He has more than 100 publications, including over 60 journal papers, over 70 conference papers, and five book-chapters. He has been serving as a Reviewer for *Automatica*, the IEEE TSMCA, the IEEE TSMCC, the IEEE TRANSACTIONS ON AUTOMATION SCIENCE AND ENGINEERING, the IEEE TRANSACTIONS ON INDUSTRIAL ELECTRONICS, *IET Control Theory and Application*, *IET Intelligent Transport Systems*, the *International Journal of Production Research*, *Computer Journal*, *the International Journal of Advanced Manufacturing Technology* (IJAMT), the *American Journal of Cardiology* (AJC), the *Journal of the Chinese Institute of Engineers* (JCIE), and the *Journal of Information Science and Engineering* (JISE). He is serving as an Associate Editor for the IEEE TRANSACTIONS ON INTELLIGENT TRANSPORTATION SYSTEMS.

Yi-Shun Weng received the B.S. degree in electrical engineering from the National Taipei University of Technology, Taipei, Taiwan, the M.S. degree from the Institute of Maritime Technology, National Taiwan Ocean University, Keelung, Taiwan, in 2000, and the Ph.D. degree in electrical and electronic engineering from National Defense University, Taiwan, in 2011.

He is currently an Associate Professor with the Department of Electronic Engineering, Army Academy, Taoyuan, Taiwan. His research interests include Petri nets, discrete event systems, and intelligent transportation systems.